

# DESIGN AND TEST OF AIR-SUCTION PEPPER SEED METERING DEVICE BASED ON AIR SUPPLY AND QUANTITATIVE SEED SUPPLY

## 基于气送定量供种的气吸式辣椒排种器设计与试验

Kaixing Zhang<sup>1)</sup>, Lan Zhang<sup>1)</sup>, Yang Ding<sup>1)</sup>, Xianxi Liu<sup>1,3)</sup>, Xiuyan Zhao<sup>\*2)</sup> 1

<sup>1)</sup> College of Mechanical and Electronic Engineering, Shandong Agricultural University, Shandong / China;

<sup>2)</sup> College of Information Science and Engineering, Shandong Agricultural University, Shandong / China;

<sup>3)</sup> Shandong Provincial Engineering Laboratory of Agricultural Equipment Intelligence, Shandong / China;

Tel: +86 13954895451; E-mail: zhaoxy@sdau.edu.cn

Corresponding author: Xiuyan Zhao

DOI: <https://doi.org/10.35633/inmateh-64-34>

**Keywords:** agricultural mechanization engineering; pepper seeds; pneumatic; quantitative seed supply; seeder

### ABSTRACT

In order to solve the problem that the current precision seeder has difficulty in precision sowing pepper seeds, an air-suction pepper seed metering device based on air supply and quantitative seed supply was developed. Combined with its basic structure and working principle, the CFD-DEM coupling method was used for analysis, and the best combined hole parameters were obtained. A single factor experiment with the pass rate, replay rate, and missed rate as experimental indicators was designed. Regression model was established to obtain a reasonable range of each parameter. The results showed that when the speed of the drum barrel was 28.65r/min and the working negative pressure was 4.40kPa, the seeding pass rate of the seed meter was 91.32%, the replay rate was 4.51%, and the missed rate was 4.17%. The comprehensive performance index was better.

### 摘要

针对目前精密排种器难以对辣椒种子进行精密播种的问题, 本文设计一种基于气送定量供种的气吸式辣椒排种器。结合其基本结构与工作原理运用 CFD-DEM 耦合方法进行分析, 获得了最佳组合型孔结构。以合格率、重播率、漏播率为实验指标, 设计单因素试验。通过正交试验建立回归模型, 得到排种性能好时各参数的合理范围。实验结果表明: 当滚筒转速为 28.65r/min, 工作负压为 4.40kPa 时, 排种器排种合格率为 91.32%, 重播率为 4.51%, 漏播率为 4.17%, 排种性能好。

### INTRODUCTION

Pepper is one of the most widely planted vegetables in China, and its annual output value ranks first among all kinds of vegetables (Xia *et al.*, 2017; Wang *et al.*, 2016). Pepper planting in China mainly relies on manual transplanting, which has low sowing efficiency and high cost, and it is only suitable for small-area planting. Therefore, the manufacture of precision pepper metering devices is of great significance to the further promotion of pepper planting (Shu *et al.*, 2018).

According to the stricter planting requirements of pepper, the best method of direct seeding of pepper is precision seeding. Cao *et al.*, (2014), used EDEM to simulate and analyse the seed trajectory, then, obtained the appropriate hole size, and designed a new type of centrifugal precision seed metering device to avoid the problem of clogging of the seed hole. Chen and Li, (2002), studied the law of seed motion in the process of supplying seeds under the action of vibration force through theory and test. Karayel *et al.*, (2004), determined the vacuum negative pressure requirements when sowing different vegetable seeds by exploring a variety of vegetable seeds. The QRIETTA air-suction vegetable planter produced by MASCHIO adopts a high-precision metering device and reduces the planting point at the same time, which realizes the precision hole planting operation for smallest seed vegetables (Guan *et al.*, 2018; Qi and Xiang, 2020).

Although the above research has made breakthroughs in different types of small particle metering devices, due to light texture and the short kidney flat structure of pepper, the above seeding device is not suitable for sowing pepper seeds (Ding *et al.*, 2018).

<sup>1</sup> Kaixing Zhang, Prof. Ph.D.; Lan Zhang, M.S. Stud.; Ying Ding, M.S. Stud.; Xianxi Liu, Prof. Ph.D.; Xiuyan Zhao, Prof. Ph.D.

Based on this, this paper designed a new type of precision seed metering device with screw conveying and air conveying combined seed feeding and negative pressure suction, and determined the optimal combination parameters through simulation and bench test. The research in this paper can provide a theoretical basis for the design and improvement of pepper seeding device and optimization of motion parameters.

## MATERIALS AND METHODS

### *The overall structure and working principle of the seed metering system*

#### *The whole frame*

The structure diagram of the air-suction pepper metering device is shown in Fig. 1.

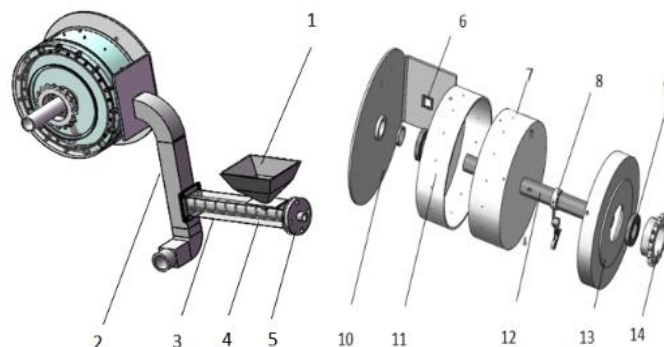


**Fig. 1 - Overall structure of the seed metering system**

1 - Feed hopper; 2 - Air flow seed tube; 3 - Spiral roller shell; 4 - Spiral roller blowing nozzle; 5 - End cap; 6 - Ferrule; 7 - Inner tube; 8 - Seeding wheel; 9 - Sealed bearing; 10 - Seed shell scraper; 11 - Seed shell; 12 - Seeding axis; 13 - Back shell; 14 - Sprocket

The air-suction pepper seed metering device is mainly composed of spiral rollers, inner and outer cylinders, rear shell, air flow seed tube, seed suction shell, seed metering wheel, seed metering shaft, feeding hopper and other components.

#### *The working principle*

During operation, the pepper seeds enter the spiral conveying mechanism through the seed box, and enter the air flow seed tube with the rotation of the spiral roller. Under the action of the air blowing force, the seeds are blown near the suction nozzle of the drum. Under the action of negative pressure, the seeds are absorbed by the seed suction holes on the drum machine and rotate with the drum. When the seeds turn to the position of the seeding wheel, the suction holes lose their adsorption force to the seeds. Under the action of gravity and centrifugal force, the seeds fall into the seed bed at a certain speed, and finally complete the seeding process.

#### *Back shell structure design*

The back shell structure is shown in Fig. 2, the blue part is the inner negative pressure cavity, and the yellow is the outer negative pressure chamber. Inside the disc, weld an annular welding plate with a diameter of 160mm concentric with the disc and a height of 13mm. A vent hole with a diameter of 4mm is opened on the annular welding plate to realize the connection of the internal and external negative pressure chambers. Part of the internal negative pressure chamber is welded with partition ribs of 4mm×10mm×10mm in length, width and height respectively. The internal negative pressure chamber is divided into separate isolated negative pressure chambers. The partition ribs are uniformly welded every 24°, and each isolated negative pressure chamber corresponds to a seed suction hole on the circumference of the inner and outer cylinders, and the pressure of each seed suction hole does not affect each other, which makes the air pressure at the seed suction nozzle more stable and avoids the negative pressure turbulence at the suction nozzle caused by unstable airflow.

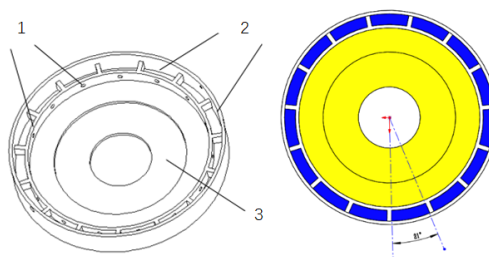


**Fig. 2 - Design of the rear shell structure**

1 - Vent hole; 2 - Isolated negative pressure chamber; 3 - Negative pressure chamber

**Inner and outer cylinder structure design**

The structure of the inner and outer cylinders of the seed metering device is shown in Fig. 3. The inner cylinder and the outer cylinder are nested with each other, and the vent holes on the inner and outer cylinders are aligned with each other. The inner cylinder is designed with uniformly distributed L-shaped negative pressure flow passages with a diameter of 1.5mm. Each L-shaped flow channel communicates with the internal negative pressure cavity on the rear shell to form a separate negative pressure flow channel. This single flow channel structure design makes the airflow of each seed suction hole affect the seed suction effect independently when the seed enters the seed metering device from the seed suction hole, ensuring the stability of the seed suction and seed carrying process.

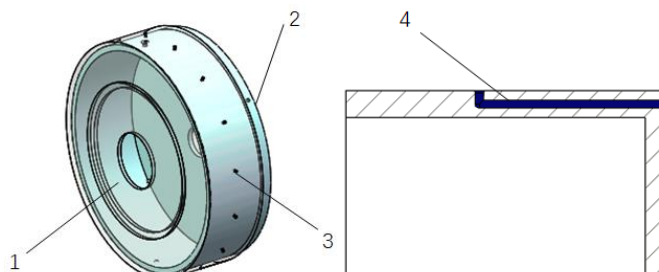


**Fig. 3 - Structure of inner and outer cylinders**  
 1 - Outer tube; 2 - Inner tube; 3 - Seed suction hole; 4 - Inner tube runner structure

**Screw conveyor**

The screw conveying mechanism is a mechanism that controls the amount of seed in the process of feeding. When the pitch is constant, the conveying capacity of the screw conveyor is mainly related to factors such as speed, screw diameter, and blade shape. The speed of screw conveying should be based on the conveying volume and screw. The diameter and the characteristics of the material are determined. The blade speed should not be too high when the conveying requirements are met, and it should not exceed the maximum allowable speed. The spiral speed is calculated using Eq.(1):

$$n \leq n_{max} = \frac{A}{D} \frac{1}{2} \tag{1}$$

where:

A is material characteristic coefficient, A=20; D is spiral diameter, [m].

The size of the pitch s determines the lift angle of the spiral blade, so the pitch directly affects the slip surface of the seed material, and then affects the conveying capacity of the screw conveying mechanism. Two conditions should be met in the design and calculation of the pitch: one is to ensure the proper distribution relationship between the components of the speed; the other is to consider the frictional connection between the spiral body and the material, and the pitch is calculated using Eq. (2):

$$s = (0.8 \sim 1.2) D = kD \tag{2}$$

Given the spiral diameter D=24mm, the maximum allowable speed n<sub>max</sub>=130r/min and the pitch s=19~28.8mm can be calculated. In this paper, the thread pitch is selected as 20mm, and the distance for the spiral seeding is 157mm, as shown in Fig. 4.

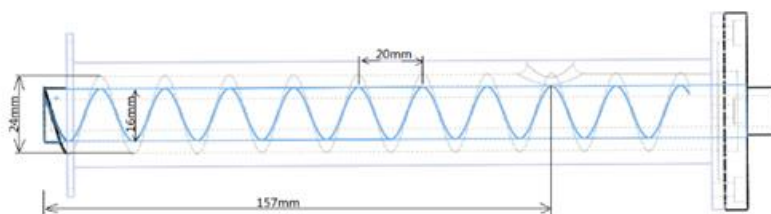


**Fig. 4 - Structural design of spiral conveying**

**Optimization Simulation Analysis of Seed Metering Device**

Based on the structural design of the seed metering system, CFD and DEM simulation are used to select the optimal seed blowing speed, and to verify the rationality of the structural parameters for seed feeding and seeding (Ji et al., 2018). The grid division of positive and negative pressure flow fields is shown in Fig. 5.

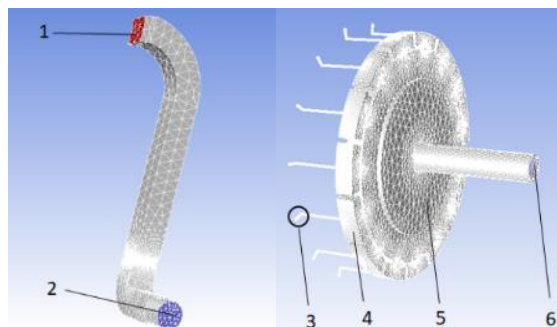


**Fig. 5 - Meshing of positive pressure flow field and negative pressure flow field**  
 1 - Positive pressure outlet; 2 - Positive pressure inlet; 3 - Suction nozzle; 4 - Internal negative pressure cavity; 5 - External negative pressure cavity; 6 - Negative pressure inlet

**Optimal selection of suction hole structure**

The roller of the seed metering device adopts a double-layer roller structure, combined with the special shape of pepper seeds, optimized on the basis of the single-layer roller suction hole structure, and designed stepped holes, tapered holes, straight one holes, and straight two holes. There are four types of holes. Use FLUENT fluid simulation to select a seed suction hole structure with uniform pressure and velocity distribution and appropriate values.

Define the flow velocity of the air inlet when the negative pressure is 4.5kPa, and the flow velocity of the inlet is 10m/s. The flow channels of different holes are simulated, and the pressure velocity distribution obtained is shown in Fig. 6. On the whole, the stepped hole produces a larger turbulent flow at the nozzle. The overall velocity and pressure distribution of the straight hole is relatively uniform, but the flow rate is small, and the power consumption is large. Obviously these two types of holes are not suitable for the seed suction holes of the seed metering device. The cloud diagram of pressure and velocity distribution of straight two holes and tapered holes are the same except for the nozzle. Taking into account the actual situation, although the tapered hole has a small part of turbulence at the nozzle, the tapered hole is more beneficial for the adsorption of pepper seeds. The shape of the suction hole is finally determined to be a tapered hole.

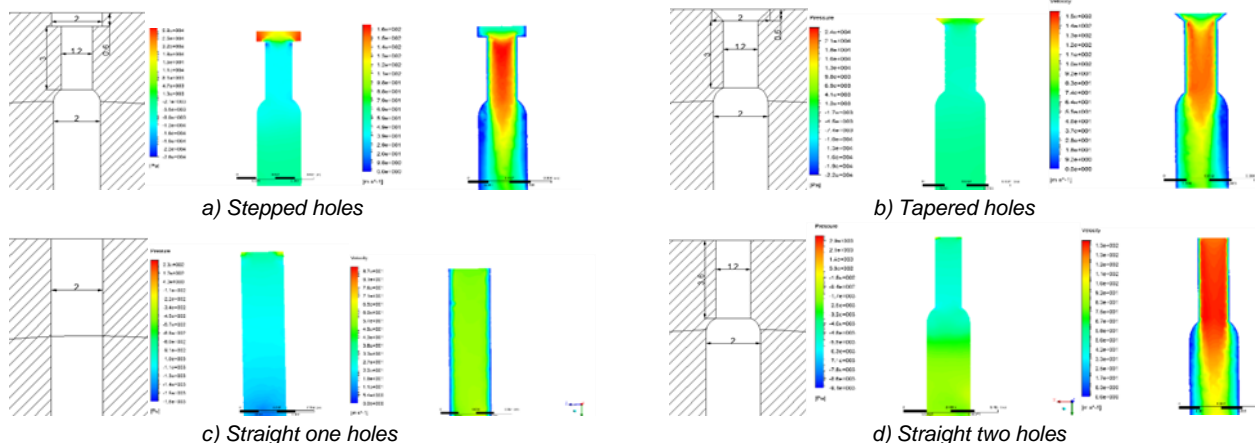


**Fig.6 - Cloud diagram of pressure velocity of different shaped holes**

**EDEM simulation analysis of seed supply process**

This article uses EDEM 2018 and FLUENT17.0 for simulation, and couples EDEM and Fluent through journal files. The CFD-DEM simulation parameters are shown in Table 1.

**Table 1**

EDEM simulation parameter setting		
material	Pepper seeds	steel
Poisson's ratio	0.3	0.3
Shear modulus	1.0e+06Pa	8.3e+10Pa
Density	461kg/m <sup>3</sup>	7890kg/m <sup>3</sup>
Collision recovery factor (with particles)	0.35	0.6
Static friction coefficient (with particles)	0.3	0.3
Dynamic friction coefficient (with particles)	0.01	0.12

In the spiral conveying stage, the force and trajectory of the particles are basically stable, which is mainly manifested in the interaction between the particles and the interaction between the blades and the particles. After many simulations, it was concluded that the speed of the spiral blade is relatively low, so the seeds in the seed feeding process were basically concentrated in the lower part of the blade, and the conveyed particles were divided into different parts by the blade, one rotation of the spiral blade could provide 80 seeds. Analysing the force of 4 particles at different positions during the spiral conveying process, the maximum force was 0.013N, 0.00034N, 0.0007N, 0.00045N, which would not damage the seeds; the speed of the particles when they finally collided with the drum was between 0.8m/s~1m/s; although the particles had a rebound effect after collision, they met the requirements of seeding, which were within the effective adsorption and seeding distance. Seed supply process and seed stress were shown in Fig. 7.

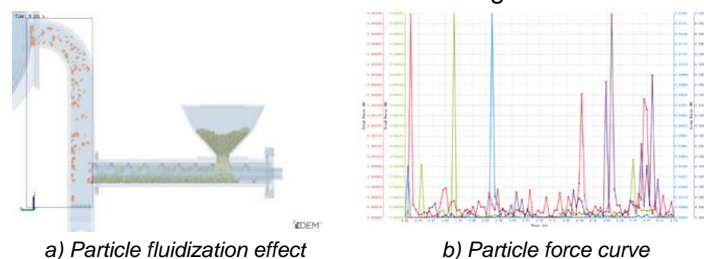


Fig. 7 - Particle velocity analysis

### CFD simulation study of suction flow field

The air pressure inside the suction drum and the stability of the internal air flow affect the seed suction effect. Define the simulated negative pressure of the flow field as 4kPa, use the slipping grid command to define the rotation vector for the negative pressure boundary as (0, 0, 1), the speed is 4 rad/s, and analyse the distribution of velocity, turbulence velocity, dynamic pressure, and static pressure at different sections and times in the flow field, and output the distribution of the flow field  $z=2\text{mm}$ ,  $z=5.5\text{mm}$  and  $z=45\text{mm}$  in the drum at 0.01s, 0.1s and 1s. The results are shown in Fig. 8.

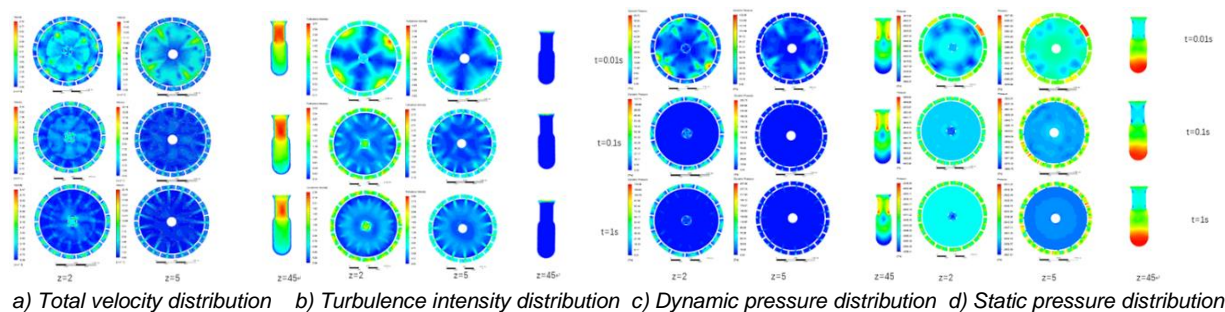


Fig. 8 - Velocity and turbulent intensity distribution of the channel

It can be seen from Fig. 8 that the velocity, turbulence, dynamic pressure and static pressure distribution of the negative pressure chamber were significantly affected by the air inlet when the simulation was 0.01s, and there was also a phenomenon of negative pressure concentration. According to Fig.8a), the flow velocity of the negative pressure chamber was weakened by the influence of the air inlet at 0.1s, and the flow velocity and turbulence also tended to be stable; at 1s, the flow velocity of the internal negative pressure chamber had reached a relatively stable state, and the specific performance was that the flow velocity of the external negative pressure chamber was basically in the range of 0m/s~5m/s. According to Fig.8c), the dynamic pressure of the inner and outer negative pressure chambers had stabilized at 0Pa during the two stages of  $t=0.1\text{s}$  and  $t=1\text{s}$ . During the 0.01s~1s of the simulation, the values at the seed suction holes had been kept in a stable state, the flow velocity was maintained between 30m/s~40m/s, and the negative pressure could reach about 250Pa. According to force formula: force = pressure x force area ( $F=P \cdot S$ ), the suction was about 0.079N, which met the suction requirements of pepper seeds.

In general, the negative pressure flow channel of the flow field is small in size, the stable time is shortened, and the suction force at the seed suction nozzle better meets the requirements. After the flow field is stable, the pressure in the inner negative pressure chamber is higher than that in the outer negative pressure chamber, which can save pressure and reduce power consumption.

**RESULTS AND DISCUSSION**

**Bench Test of Air-Suction Pepper Metering System**

**Test material**

Two gold bars of pepper seeds were selected as the test object, and the seed metering test was conducted in the performance test of the JPS-12 seed metering device. The seed purity was >98%, the water content was <7%, and the plant spacing was 300mm/plant, the test was shown in Fig. 9.



**Fig. 9 - Seed Meter Performance Tester**

1 - High-speed camera; 2 - transmission shaft; 3 - Seed metering device; 4 - Negative pressure tube; 5 - Seed tube

**Single factor test analysis**

In order to explore the influence of the negative pressure and speed of the seed metering device on the seed metering performance, some researchers first conducted a single factor test on the seed metering device (Yang et al., 2015). This test researched working performance of the seed metering device under a forward speed of 7km/h, a drum speed of 25.9r/min, and negative pressure of 1.5~5.5kPa. It could be obtained from the test that during the process of working negative pressure from 1.5kPa to 3.5kPa, the pass rate showed a gradual upward trend, which was mainly manifested in the decrease of missed rate and increase of replay rate. The pass rate of negative pressure in the process of 3.5kPa to 5kPa tended to be stable. When the negative pressure was greater than 5kPa, the missed rate dropped rapidly, and the replay rate raised rapidly. Considering comprehensively, the seeding effect was good when the negative pressure range was 3.5~5kPa.

The rotation speed of the seed meter is determined by the seeding interval and the machine's forward speed, and the conversion relationship is shown using Eq. (3):

$$n_p = \frac{60 \times 10^3 v_m}{3.6 \cdot S \times Z} \tag{3}$$

where:

$v_m$  is the forward speed of the planter, [km/h];

$S$  is plant spacing;

$Z$  is number of seeding disc holes,  $Z=15$ .

On the basis of the negative pressure single factor test, the negative pressure 4kPa with the highest pass rate is selected as the working pressure of the speed single factor test. Select the seed metering device speed and drum speed as shown in Table 3 and observe the seeding effect. The test results are shown in Table 3. Take the pass rate (coded value A), replay rate (coded value D), and missed rate (coded value M) as the test indicators. According to the test, during the process of increasing the working speed from 3 km/h to 5km/h, the pass rate showed a gradual downward trend, mainly manifested in the rapid increase of the missed rate and the slow decline of the replay rate. When the working speed increased from 5km/h to 9km/h, the pass rate tended to be stable; when the speed was greater than 9km/h, the replay rate remained unchanged, the missed rate gradually increased, and the pass rate showed a downward trend. Considering comprehensively, when the forward speed was 5-9km/h, the drum speed was 18.5-33.3 r/min, the seeding effect was good.

**Table 2**

Pressure single factor test results									
Negative pressure (kPa)	-1.5	-2	-2.5	-3	-3.5	-4	-4.5	-5	-5.5
Missed rate (M %)	15.62	14.32	12.98	12.21	9.65	8.11	7.6	7.12	4.11
Replay rate (D %)	1.6	2.41	2.82	3.2	3.29	3.87	4.54	5.69	10.24
Pass rate (A%)	82.78	83.27	84.20	84.59	87.06	88.02	87.86	87.19	85.76

Table 3

Speed single factor test results										
Speed of work (km/h)	3	4	5	6	7	8	9	10	11	12
Missed rate (M %)	2.34	4.77	7.82	7.16	8.11	7.2	8.6	9.86	10.12	13.11
Replay rate (D %)	6.37	5.78	4.15	3.41	3.87	3.34	3.76	2.64	3.54	3.72
Pass rate (A %)	91.29	89.45	88.03	89.43	88.02	89.46	87.64	87.5	86.34	83.17

**Orthogonal test analysis**

In order to further explore the interaction and influence law of negative pressure and rotation speed on the seed metering performance of the seed metering device (QI,2014), this paper carried out an orthogonal test. According to the single factor test results, the negative pressure range of the selected seed meter is 3.5~5kPa, and the forward speed range is 5-9km/h. The test factor codes are shown in Table 4 (Cheng et al., 2020).

Table 4

Factors and levels of orthogonal tests					
Factor	Level				
	1	2	3	4	5
Work negative pressure (kPa)	3.5	4	4.5	5	5.5
Forward speed (km/h)	5	6	7	8	9

**Analysis of test results**

There are 16 groups of orthogonal tests. In order to comprehensively consider the interaction between factors, each group of tests is repeated 3 times, and the data is averaged. Each test handles no less than 200 seeds. The test results are shown in Table 5.

According to Table 6, the pass rate model of the seed metering device was  $P < 0.0001$ , and the influence was extremely significant; the lack of fit item  $P = 0.7044$  ( $P > 0.05$ ), the influence was not significant. It showed that within the scope of the test data, the regression model of pass rate had a high degree of fit with the actual seeding situation. In this model, the regression terms A, AB, A2, and B2 had  $P < 0.0001$ , which was extremely significant. Missed rate model  $P < 0.0001$ , the impact was extremely significant; the lack of fit item  $P = 0.9648$  ( $P > 0.05$ ), the impact was not significant, indicating that there was no lack of fit factor in the test data interval the regression model of missed rate had a high degree of fit with the actual seeding situation (Wang et al., 2019). The replay rate model  $P < 0.0001$ , the impact was extremely significant; the lack of fit item  $P = 0.7880$  ( $P > 0.05$ ), the impact was not significant, indicating that there was no lack of fit factor in the test data interval, the regression model of replay rate had a high degree of fit to the actual seeding situation (Zheng et al., 2019).

Use Design-Expert 10.0 software to perform regression fitting on the test data. The response functions of the missed rate, replay rate and pass rate of the seed meter are  $Y_1$ ,  $Y_2$ , and  $Y_3$  respectively, and establish a regression mathematical model with the coding of each influencing factor as the independent variables. The regression model of the influence of each factor level on the missed rate, replay rate and pass rate obtained by regression fitting is as follows:

$$\begin{cases} Y_1 = +14.09714 - 1.34467A - 4.27610B - 0.12019AB + 0.31166A^2 + 0.58847B^2 \\ Y_2 = +7.88255 - 1.14807A - 2.43898B - 0.093917AB + 0.22731A^2 + 0.67454B^2 \\ Y_3 = +78.05154 + 2.47395A + 6.69169B + 0.23097AB - 0.54362A^2 - 1.26431B^2 \end{cases} \quad (4)$$

After excluding the insignificant regression, the regression model of pass rate, missed rate and replay rate can be expressed as:

$$\begin{cases} Y_1 = +14.09714 - 1.34467 A - 4.27610 B - 0.12019 AB + 0.31166 A^2 + 0.58847 B^2 \\ Y_2 = +7.88255 - 2.43898 B - 0.093917 AB + 0.22731 A^2 + 0.67454 B^2 \\ Y_3 = +78.05154 + 2.47395 A + 0.23097 AB - 0.54362 A^2 - 1.26431 B^2 \end{cases} \quad (5)$$

Table 5

Orthogonal test results

Test number	Test factors		Evaluation index			Test number	Test factors		Evaluation index		
	Forward speed A(km/h)	Work negative pressure B (kPa)	Missed rate Y <sub>1</sub> (%)	Replay rate Y <sub>2</sub> (%)	Pass rate Y <sub>3</sub> (%)		Forward speed A(km/h)	Work negative pressure B (kPa)	Missed rate Y <sub>1</sub> (%)	Replay rate Y <sub>2</sub> (%)	Pass rate Y <sub>3</sub> (%)
1	4	2	6.6	3.83	89.57	9	5	5	5.51	10.05	84.44
2	5	1	10.83	6.15	83.02	10	1	5	5.88	10.1	84.02
3	1	1	9.11	4.97	85.92	11	3	5	4.32	10.24	85.44
4	5	5	5.5	9.73	84.77	12	3	3	4.1	3.95	91.95
5	3	3	4.05	3.98	91.97	13	3	5	4.47	10.58	84.95
6	1	3	5.24	6.2	88.56	14	2	4	3.8	6.89	89.31
7	1	3	5.1	6.12	88.78	15	4	4	4.2	6.21	89.59
8	1	1	9.22	5.02	85.76	16	2	2	6.5	3.52	89.98

Note: A and B are the corresponding code values of Y<sub>1</sub>, Y<sub>2</sub>, and Y<sub>3</sub>, the same below.

Table 6

Analysis of variance of orthogonal test results

Source of Variance	Missing rate Y <sub>1</sub> (%)				Replay rate Y <sub>2</sub> (%)				Pass rate Y <sub>3</sub> (%)			
	sum of square	Degree of freedom	F	P	sum of square	Degree of freedom	F	P	sum of square	Degree of freedom	F	P
A	0.76	1	63.89	0.003	0.23	1	4.34	0.0640	1.84	1	92.41	<0.0001
B	35.08	1	2935.73	<0.0001	38.01	1	729.24	<0.0001	0.055	1	2.76	0.1274
AB	1.04	1	87.16	0.0003	1.05	1	20.15	0.0012	4.18	1	209.62	<0.0001
A2	2.64	1	220.70	<0.0001	1.33	1	25.59	0.0005	7.62	1	382.46	<0.0001
B2	15.12	1	1265.57	<0.0001	12.60	1	241.77	<0.0001	55.62	1	2792.01	<0.0001
Model	63.79	5	1067.74	<0.0001	74.53	5	286.02	<0.0001	107.82	5	1082.40	<0.0001
Residual	0.12	10			0.52	10			0.20	10		
Lack of fit	0.017	5	0.17	0.9648	0.17	5	0.47	0.7880	0.075	5	0.60	0.7044
Error	0.10	5			0.36	5			0.12	5		
Sum	63.91	15			75.06	15			108.02	15		

Note: P<0.05 (significant impact), P<0.01 (very significant), P>0.25 is not significant.

Two-factor interaction analysis

In order to more intuitively analyse the relationship between the various influencing factors and performance of the seed metering device, and to seek the best combination of operating parameters, the test data is further processed through the Design-Expert 10.0 software to obtain the response surface diagram of the interactive factors (Gao et al., 2019). It could be found from Fig.10 that the interactive factors had a significant impact on the missed rate, replay rate and pass rate (Ding et al., 2018; Liu et al., 2019).

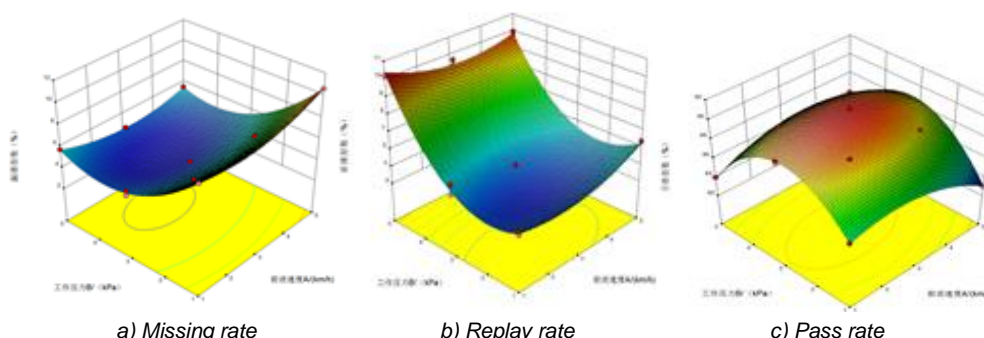


Fig. 10 - Interactive factor response diagram

It could be seen from Fig.10a) that the missed rate decreased first and then increased slightly with the increase of working negative pressure, while the missed rate first decreased and then increased during the change of forward speed, with a small change. It could be seen from Fig.10b) that the replay rate first increased slightly and then increased greatly with the increase of the working negative pressure, while the replay rate first decreased and then increased as the forward speed increased, with a small change.

It could be seen from Fig.10c) that the pass rate first increased and then decreased during the process of increasing working negative pressure and forward speed, and the changes were obvious. Among them, when the forward speed of the seed meter is 6~8km/h, that is, when the rotating speed is 22-30 r/min and the working negative pressure is in the range of 4kPa~5kPa, the missed rate and replay rate of the seed metering device are at a low level, while the pass rate is at a high level. Based on comprehensive consideration, the best optimized parameters of the seed metering device are: forward speed 7.72km/h, that is, the drum speed is 28.56r/min, and the working negative pressure is 4.37kPa. At this time, the pass rate is 91.07% and the missed rate is 4.23. %, the replay rate is 4.70%.

The optimized theoretical results were tested and verified on the seed meter performance test bench. Here the optimized data is adjusted appropriately, the forward speed of the seed metering device is set to 7.72km/h (rotating speed is set to 28.56r/min), the working negative pressure is set to 4.40kPa and 4 repeated tests are performed. The average seeding pass rate is 91.32%, the average replay rate is 4.51%, and the average missed rate is 4.17%. The test result of the bench is basically consistent with the theoretical analysis result, which can be used as the final best working speed.

## CONCLUSIONS

(1) The innovative design of the negative pressure chamber structure inside the seed meter makes the internal negative pressure of the seed metering device more stable.

(2) The tapered hole is selected as the suction hole structure, the CFD-DEM coupling method is used to simulate the seed supply process and the air flow field of the pepper precision metering device, which proves the rationality of the structure.

(3) The best optimized parameters of the seed metering system are: the rotation speed is 28.56r/min, the negative pressure is 4.40kPa, the average seed metering pass rate of the metering device is 91.32%, the average replay rate is 4.51%, and the average missed rate is 4.17%, which meets the demand for seeding.

## ACKNOWLEDGEMENT

The study is supported by the Key Research and Development Programme (2019GNC106120) in Shandong province and "Double First-Class" Award and Supplementary Fund Project (SYL2017XTTD14) in Shandong province.

## REFERENCES

- [1] Chen J., Li Y.M., (2002). Study on the Law of Seed Movement in the Air Suction Vibration Seeding Test Bench (气吸振动式播种试验台内种子运动规律的研究). *Journal of Transactions of the Chinese Society of Agricultural Machinery*, Vol. 1, issue 33, pp: 47-50;
- [2] Cao X.Y., Liao Q.X., Cong J.L. et al., (2014). Structural design and test of centrifugal rapeseed seed metering device (离心式油菜精量排种器型孔结构设计与试验). *Journal of Transactions of the Chinese Society of Agricultural Machinery*, Vol. S1, issue 45, pp. 40-46;
- [3] Cheng C., Fu J., Hao Fu P. et al., (2020) Effect of motion parameters of cleaning screen on corn cob blocking law (清选筛运动参数对玉米芯轴堵筛规律的影响). *Journal of Jilin University. (Engineering and Technology Edition)*, Vol. 01, issue 50, pp. 351-360;
- [4] D. Karayel, Z.B. Barut, A. Özmerzi., (2004). Mathematical Modelling of Vacuum Pressure on a Precision Seeder. *Journal of Biosystems Engineering*, Vol. 4, issue 87;
- [5] Ding L., Yang L., Wu D.H. et al., (2018). Simulation and experiment of corn air suction seed metering device based on DEM-CFD coupling (基于 DEM-CFD 耦合的玉米气吸式排种器仿真与试验). *Journal of Transactions of the Chinese Society of Agricultural Machinery*, Vol. 11, issue 49, pp. 48-57;
- [6] Ding L., Yang L., Liu S.R. et al., (2018). Design of pneumatic maize seed-metering device with assistant seed filling plate (辅助充种种盘玉米气吸式高速精量排种器设计). *Journal of Transactions of the Chinese Society of Agricultural Machinery*, Vol. 22, issue 34, pp. 1-11.
- [7] Guan C.S., Cui Z.C., Gao Q.S. et al., (2018). Research Status of Precision Vegetable Live Broadcasting Technology and Equipment (蔬菜精量直播技术及装备的研究现状). *Journal of China Vegetables*, Vol. 12, pp. 9-15;
- [8] Gao X.J., Xu Y., He X.W. et al., (2019). Design and test of air-fed high-speed corn precision metering device guide turbine (气送式高速玉米精量排种器导流涡轮设计与试验). *Journal of Transactions of the Chinese Society of Agricultural Machinery*, Vol. 11, issue 50, pp. 42-52;

- [9] Ji S.M., Ge J.Q., Gao T. et al., (2018). Processing characteristics of surface-constrained soft abrasive flow based on CFD-DEM coupling (基于 CFD-DEM 耦合的面约束软性磨粒流加工特性研究). *Journal of Mechanical Engineering*, Vol. 05, issue 54, pp. 129-141;
- [10] Liu Y.Q., Zhao M.Q., Liu F. et al., (2016). Simulation and optimization of working parameters of air suction metering device based on discrete element (基于离散元的气吸式排种器工作参数仿真优化). *Journal of Transactions of the Chinese Society for Agricultural Machinery*, Vol. 7, issue 47, pp. 65 – 72;
- [11] Qi B., (2014). *Design and experimental research of central collection and exhaust precision seed metering device (中央集排气送式精量排种器设计与试验研究)*. China Agricultural University;
- [12] Qi Y.Z., Xiang S.N., (2020). Research Status and Development Trend of Vegetable Planter at Home and Abroad (国内外蔬菜播种机的研究现状与发展趋势). *Journal of Chinese Journal of Agricultural Mechanization*, Vol. 01, issue 41, pp. 205-208;
- [13] Shi S., (2015). *Design and experimental study of compressed corn precision seed metering device (气压组合孔式玉米精量排种器设计与试验研究)*. China Agricultural University;
- [14] Shu S., Kang Y.Y., Wang Y. et al., (2018). Analysis of the development, characteristics and trends of the world protected horticulture (世界设施园艺发展概况、特点及趋势分析). *Journal of China Vegetables*, Vol. 07, pp. 1-13;
- [15] Wang L.H., Fang Z.Y., Du Y.C., et al., (2016). Research on the development strategy of vegetable seed industry in China (我国蔬菜种业发展战略研究). *Journal of China Engineering Science*, Vol. 01, issue 18, pp. 123-136;
- [16] Wang Q., Zhu L.T., Li M.W. et al., (2019). Vibration characteristics of finger-tipped corn no-till precision seeder and its effect on seeding performance (指夹式玉米免耕精密播种机振动特性及对排种性能的影响). *Journal of Agricultural Engineering*, Vol. 09, issue 35, pp. 9-18;
- [17] Xia B.B., Li Y., Wang H.M., Li T., Xu X.W., Wu Z.M., (2017). Cluster Analysis of Morphological Traits of Hot Pepper Germplasm Introduced from Abroad (国外引进辣椒资源形态学性状的聚类分析). *Journal of Molecular Plant Breeding*, Vol. 08, Issue 15, pp. 3318-3330;
- [18] Zheng W.X., Lu Z.Q., Zhang W.Z. et al., (2019). Design and test of single row sweet potato seedling recovery machine (单行甘薯秧蔓回收机设计与试验). *Journal of Agricultural Engineering*, Vol. 06, issue 35, pp. 1-9.